



Supplement of

Physical drivers of the November 2023 heatwave in Rio de Janeiro

Catherine C. Ivanovich et al.

Correspondence to: Catherine C. Ivanovich (cci2107@columbia.edu)

The copyright of individual parts of the supplement might differ from the article licence.

Supplemental Figures

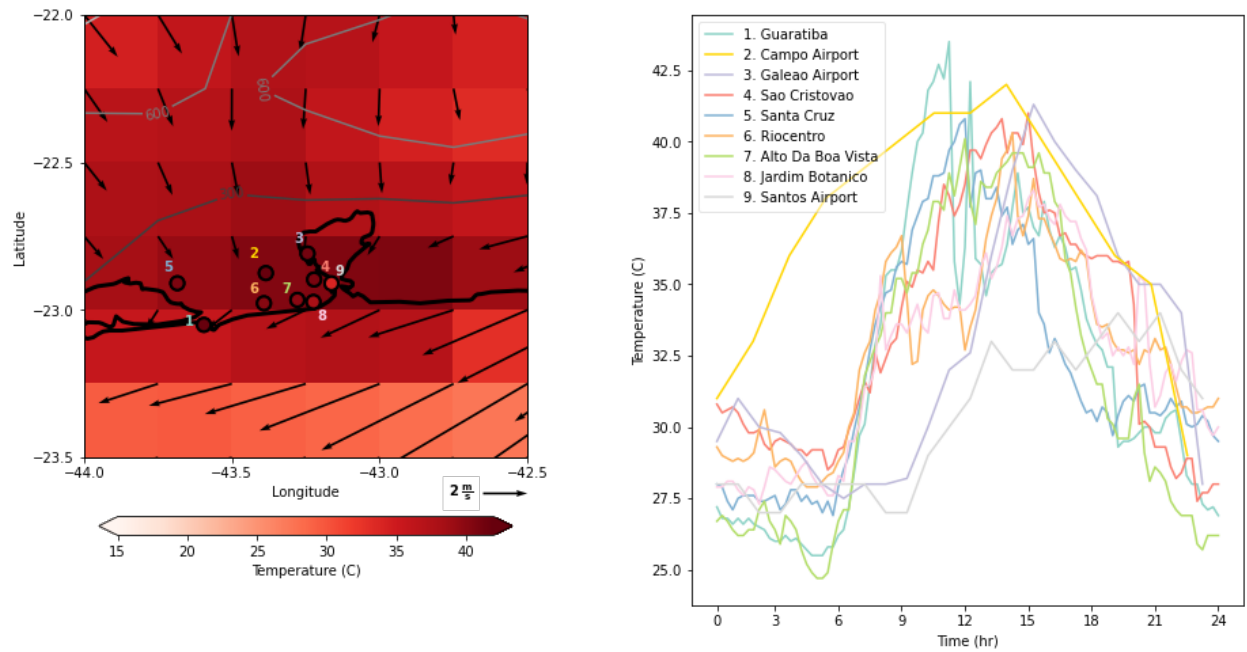


Figure S1: Spatial and temporal variability of extreme heat on November 18, 2023 measured by nine weather stations in Rio de Janeiro. Left: Spatial map of station locations colored by the maximum temperature measured on November 18 compared to ERA5 reanalysis data. Right: Time series of hourly air temperature measured at each station on November 18. Stations are listed in order from highest to lowest maximum recorded temperature.

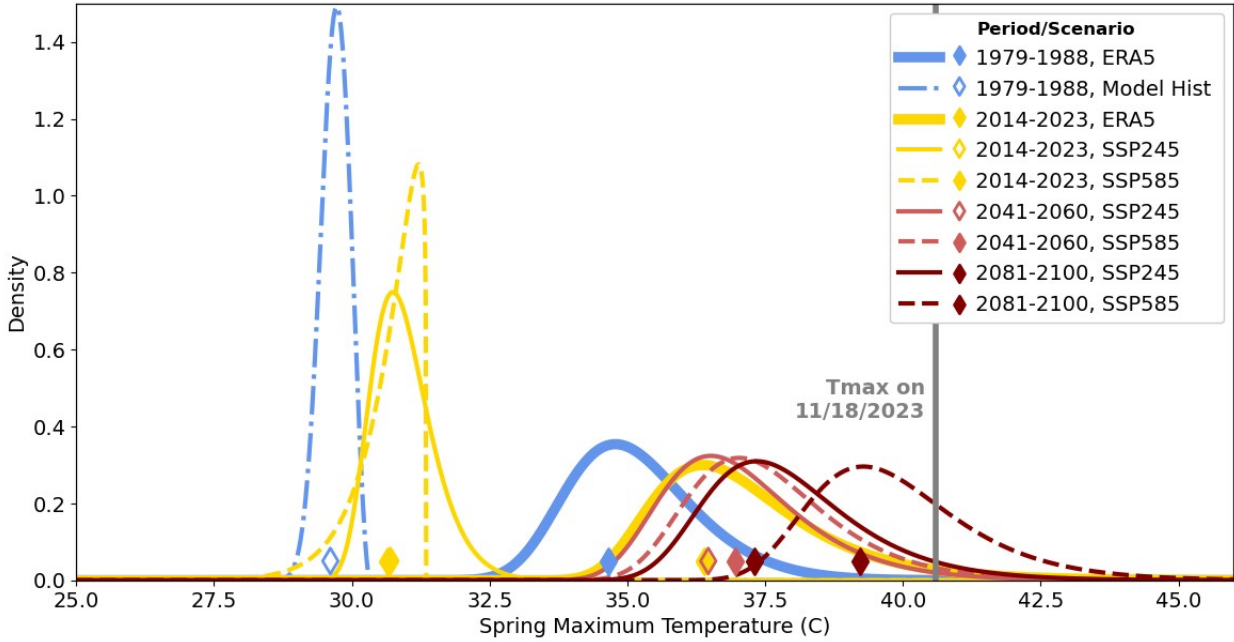


Figure S2: Same as Fig. 9, with additional comparison of GEV distributions for SON maximum temperatures during early and late historical periods in NEXGDDP model data (before bias correction). Two scenarios are shown for the late historical period, as the models switch from “retrospective” (1950-2014) to “prospective” (2015-2100) simulations during this time period.

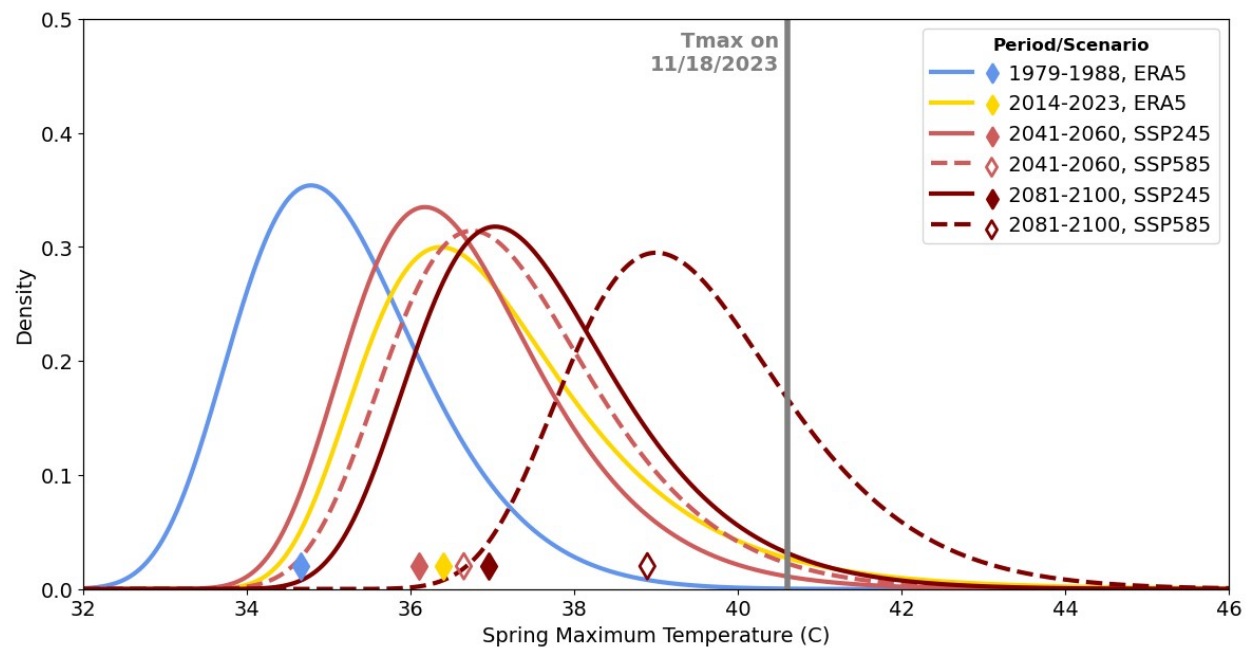


Figure S3: Same as Fig. 9, but only taking the average over the six models with a Perkins skill score above 80% compared against ERA5 during the period from 1981-2013.

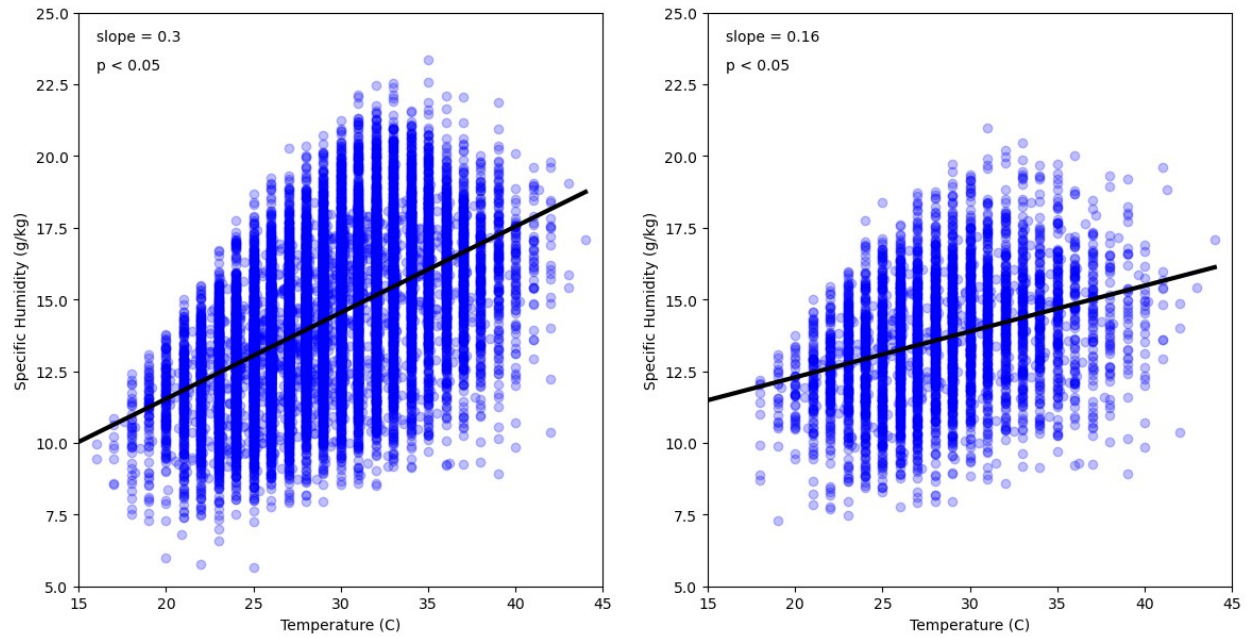


Figure S4: Correlation between daily maximum temperature and daily mean specific humidity in Rio de Janeiro for a) full year and b) SON season. Data measured by the Galeão International Airport weather station as reported by the HadISD dataset.

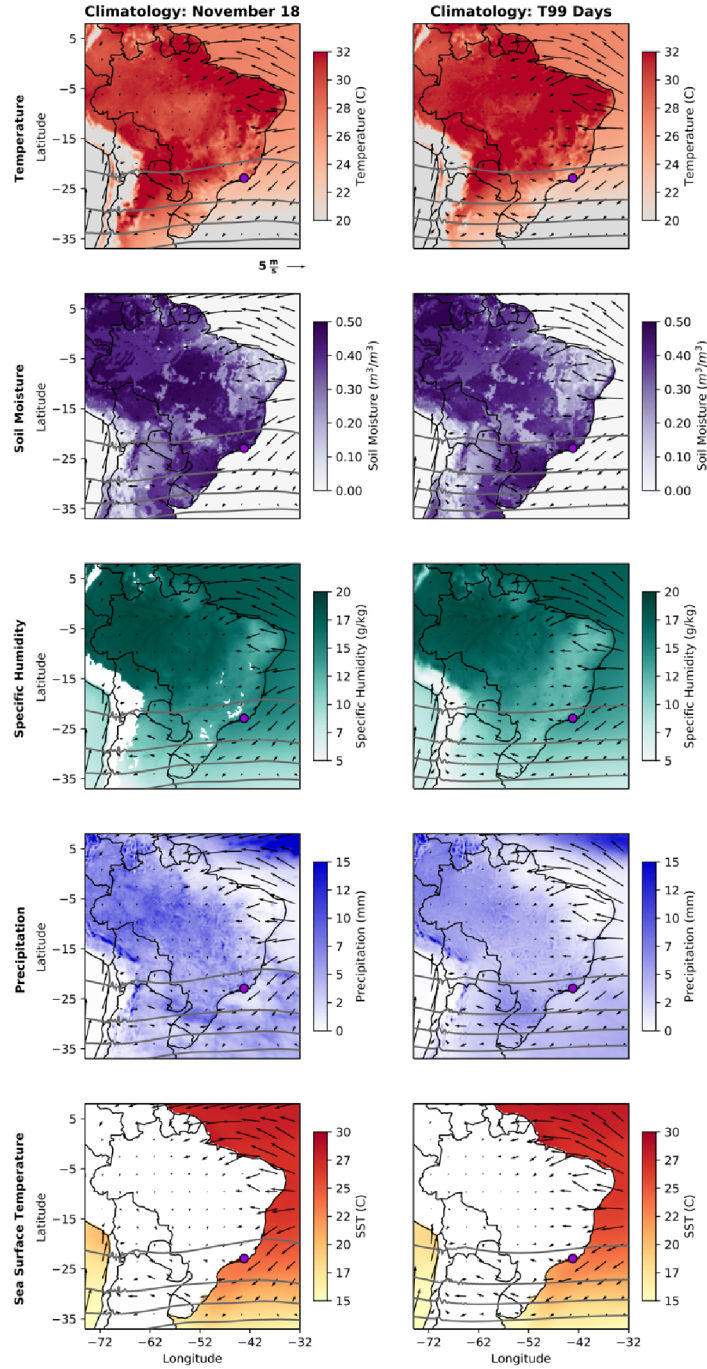


Figure S5: Analogous to Figs. 3 and 4, but showing the climatology of daily maximum temperature, mean soil moisture, mean specific humidity, total precipitation, and mean sea surface temperature on November 18 throughout the historical record (left) and on dates corresponding to 99th percentile temperature events in the city of Rio de Janeiro (right).

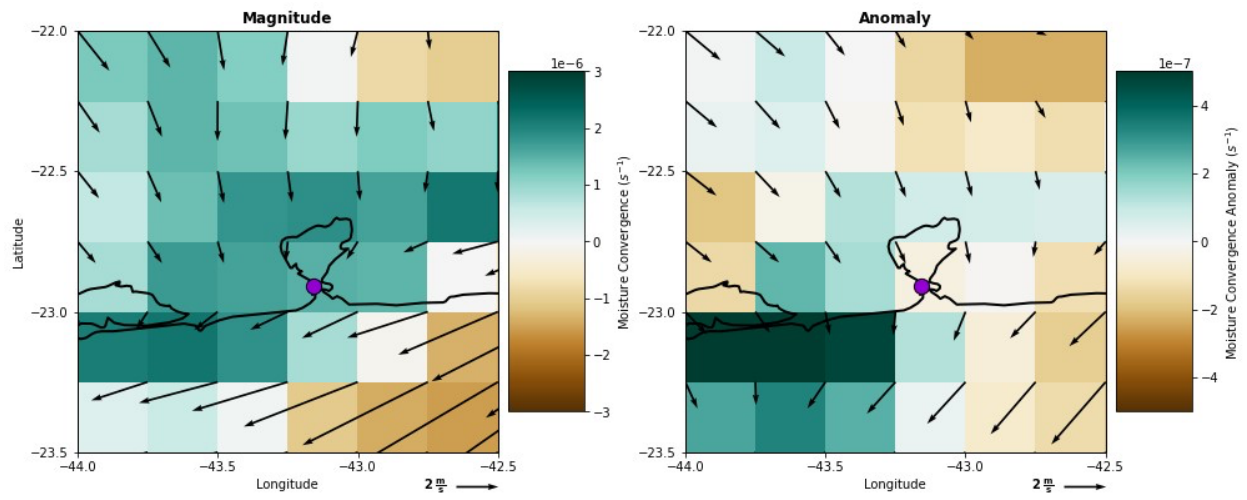


Figure S6: Surface level moisture flux convergence and wind magnitude (left) and anomaly (right). Anomalies are calculated relative to historical day-of-year average.

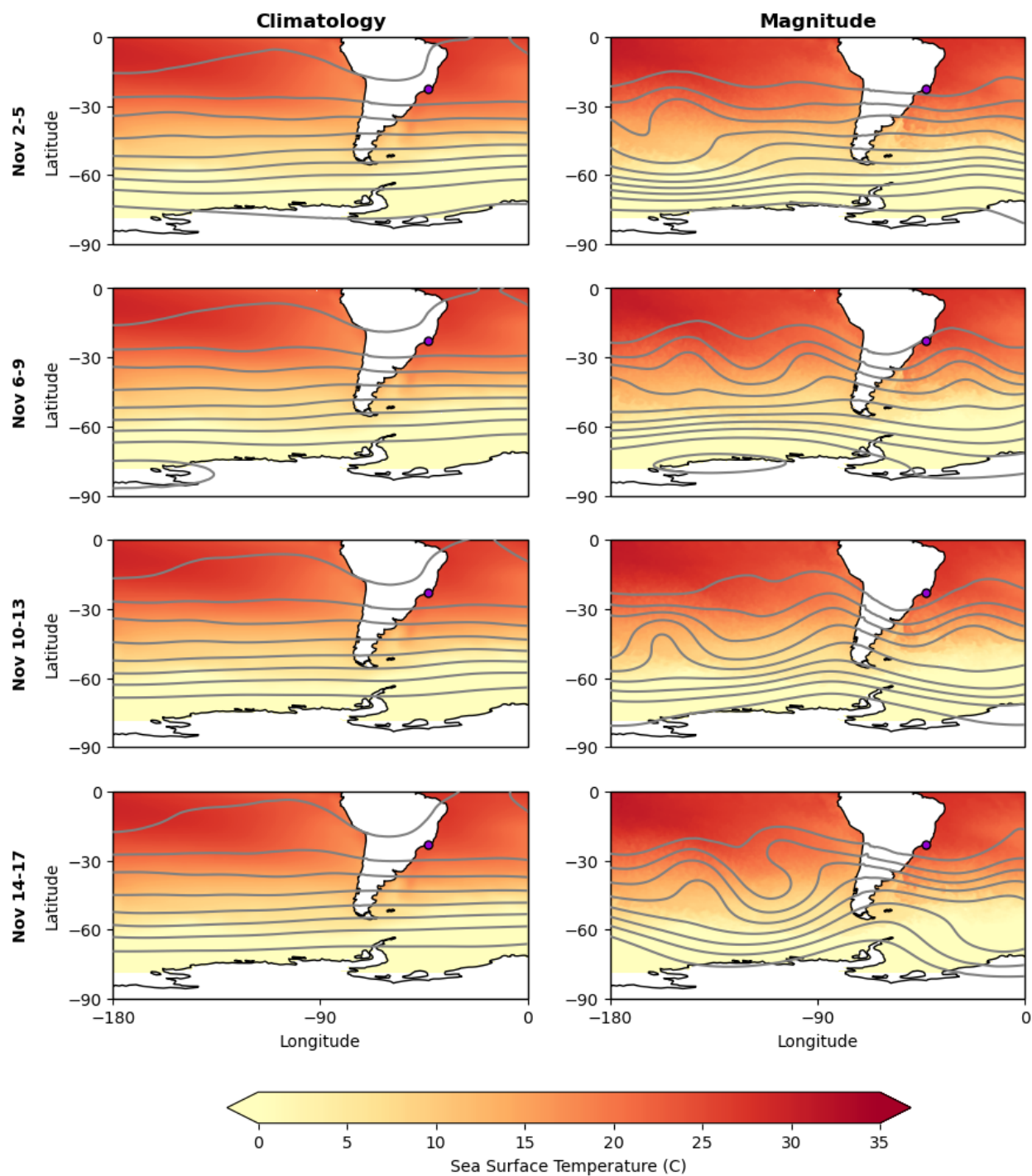


Figure S7: Analogous to Fig. 6 but showing the sea surface temperature (shading) and geopotential height at 200 hPa (contours) as the climatology for given dates in the historical period (left) and the absolute magnitude of these variables during these calendar dates in November 2023 (right).

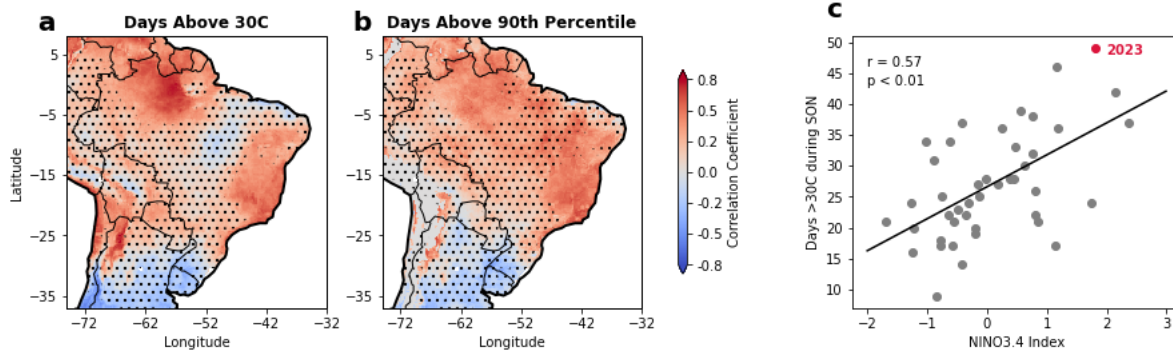


Figure S8: Historical correlation from 1979-2023 between Niño3.4 index and number of days per year above a) 30°C and b) locally defined 90th percentile. Stippling shows areas which are not significant at a $p = 0.05$ level. c) Correlation between the number of days above 30°C per year taking place in the SON season in ERA5 for the grid cell which includes the Galeão International Airport weather station and the Niño3.4 index.

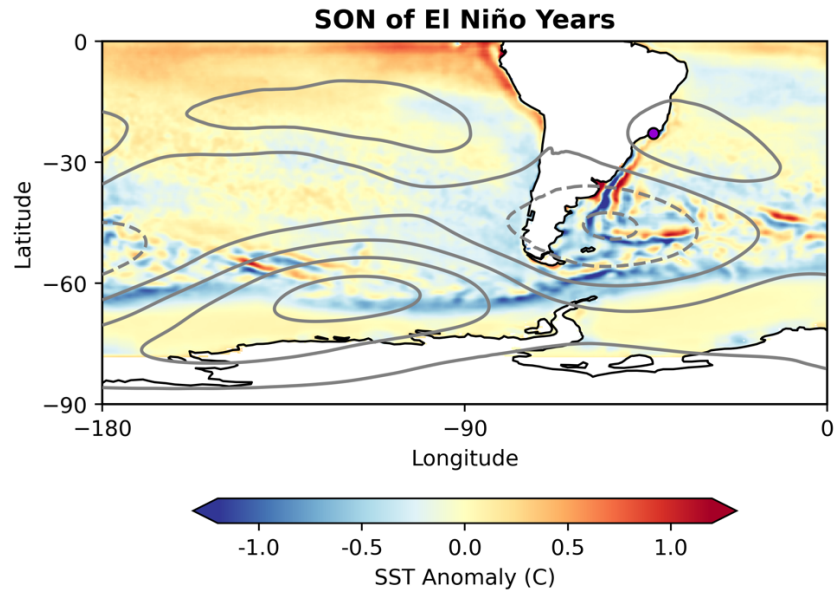


Figure S9: Mean SST anomalies (shading) and geopotential height anomalies at 200 hPa (contour) during September-November of El Niño years as defined by the Niño3.4 index. Geopotential height anomaly contour levels are at 8 m, with positive (negative) anomalies in solid (dashed) contours.